

RIS and Beamformer Optimization Using Hybrid Full-Wave Analysis in Multiuser MIMO Networks

Ziqi Liu, Wei Yu, and Sean V. Hum

The Edward S. Rogers Sr. Department of Electrical and Computer Engineering, University of Toronto,
Toronto, ON, M5S 3G4, Canada (ziqii.liu@mail.utoronto.ca)

Abstract—This paper presents an accurate modeling framework for reconfigurable intelligent surfaces (RISs) in multiple-input multiple-output (MIMO) communication systems, leveraging channel information to enhance system performance. The proposed method combines hybrid ray-tracing (RT) and full-wave analysis to derive deterministic channel responses, establishing a closed-form relationship between the communication channel matrix and the RIS’s load impedances. This accurate modeling framework enables the construction of a non-diagonal impedance matrix that effectively captures critical structural factors of the RIS, such as truncation effects and mutual coupling between elements. Building on this, an optimization framework is developed to co-optimize the RIS configuration and beamforming matrix using an alternating optimization technique, with the goal of maximizing the minimum achievable rate among multiple users. A 3×3 RIS-assisted system operating in an indoor environment is considered to validate the approach. The results reveal that integrating the optimized RIS significantly boosts the achievable rate for all users. Specifically, the user rates increase from approximately 1.91 bps/Hz in the no-RIS scenario to 2.51 bps/Hz with the optimized RIS deployed.

I. INTRODUCTION

Reconfigurable intelligent surfaces (RISs) are being explored as a promising technology in next-generation wireless communication systems, with potential to enhance the spectral and energy efficiency of multiple-input multiple-output (MIMO) systems [1]. MIMO systems, which utilize multiple antennas at both the base station (BS) and user devices are designed to exploit spatial diversity and multiplexing to achieve higher data rates and improved reliability. However, the performance of MIMO systems can be significantly limited by adverse channel conditions, such as signal fading, interference, and blockage.

RISs, composed of sub-wavelength unit cells, address these challenges by dynamically manipulating electromagnetic waves through reconfigurable components, such as PIN diodes [1] and varactor diodes [2]. By precisely optimizing their configuration and controlling their electromagnetic properties, RISs can actively shape the wireless propagation environment. In MIMO systems, deploying optimized RISs enhances communication channel capacity by improving the signal-to-interference-plus-noise ratio (SINR), and enabling more effective spatial multiplexing. These advancements drive significant benefits, including increased spectral efficiency, expanded coverage, and reduced energy consumption, establishing RISs as a promising technology for future wireless networks.

Despite their potential, several challenges arise when integrating RISs into MIMO communication systems. First, in most existing literature RISs are often modeled as arrays of phase shifters that adjust the phase shifts of reflected signals to achieve constructive or destructive interference at receiving locations [3], [4]. However, such simplified models fail to capture critical RIS structural factors, including truncation effects, and most importantly, mutual coupling between RIS elements in different states, which results in a non-diagonal impedance matrix that requires optimization. These omissions result in discrepancies between theoretical predictions and actual performance. Second, statistical channel models, such as the Rician and Rayleigh fading models [5], are often used to describe communication channels. While these models account for environmental effects, advancements now enable the derivation of deterministic, site-specific models, such as ray-tracing (RT) modeling, to provide more accurate channel representations and assist in the configuration of RIS. Lastly, existing optimization methods for RIS configuration have primarily focused on redirecting beam directions [1] or optimizing reflection coefficients [3]. A more sophisticated optimization approach is required that can co-optimize the beamformers at the BS and the RIS configuration.

To address these challenges, this work explores the integration of an RIS into a practical MIMO communication system by leveraging deterministic channel information in a sub-6 GHz frequency band. The objective is to co-optimize the RIS configuration and beamforming vectors to maximize the minimum achievable rate among users, ensuring fairness in signal quality while incorporating environmental effects. To achieve this, a hybrid technique combined RT with full-wave analysis is employed [2]. This approach enables systematic evaluation of RIS scattering properties while accurately modeling environmental effects within the communication channels. Furthermore, in this work, varactors are employed as tunable elements on the surface, offering continuous capacitance adjustment to achieve precise control over the RIS configuration. Finally, this paper adopts an alternating optimization framework that iteratively refines the RIS configuration and beamforming matrix, while adhering to practical constraints such as power limitations for transmitters and bounded varactor capacitance values. We previously proposed using the hybrid technique in a single-input single-output (SISO) system [2]. This paper extends that work to MIMO systems.

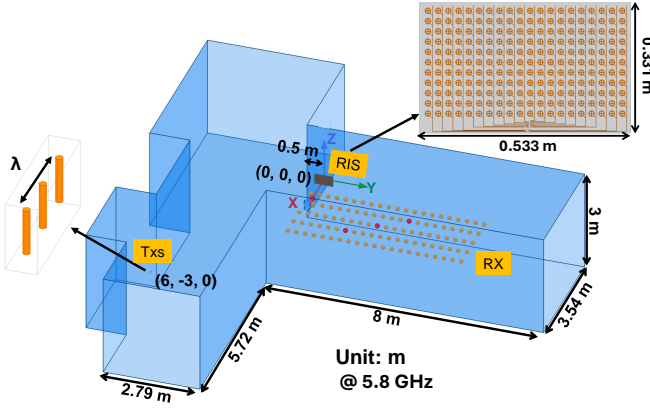


Fig. 1: Illustration of a MIMO communication environment with three linear antennas as TxS, each separated by $\lambda/2$ at an operating frequency of 5.8 GHz. The RIS is centered at $(0, 0, 0)$ with 1D control. The total electric field distribution is evaluated within the region indicated by orange dots, with the targeted users at $(1.3, 3.13, 0)$ m, $(1.8, 2.38, 0)$ m, and $(2.3, 1.63, 0)$ m, marked as red circles. Signal distributions at these locations are plotted for three different beamforming vectors, each designed to maximize the achievable rate for a specific user.

II. METHODOLOGY

This work employs a hybrid technique that combines RT with full-wave analysis to evaluate the impact of RIS in a site-specific MIMO communication system. Unlike conventional wireless communication systems, where channel state information (CSI) is typically obtained through measurements and feedback protocols [6], this approach utilizes electromagnetic shooting and bouncing ray (SBR)-based RT simulations to derive the RIS-assisted channel matrix. The process models the downlink signal propagation from the antennas at the BS, acting as transmitters (TxS), to the RIS, and subsequently to the antennas at the user terminals, acting as receivers (RxS), while accounting for environmental effects. For the simulation, a ray density of 4 rays per wavelength and a maximum of 2 bounces are assumed, chosen based on the dimensions of the RIS and the observation region to strike a balance between computational efficiency and accuracy [7]. Following this, finite element method (FEM)-based full-wave analysis is conducted using Ansys HFSS (high-frequency structure simulator) to evaluate the RIS's scattering behavior, incorporating key factors such as truncation effects, and mutual coupling. By employing the hybrid technique, we establish a closed-form relationship between the total fields in the environment and the non-diagonal impedance matrix, which accounts for mutual coupling and tunable load effects. By optimizing the load impedance, we maximize communication performance, demonstrating the effectiveness of this approach.

In this work, we consider a system involving M TxS, T field points with K user terminals positioned among the field points, and N reconfigurable elements in the RIS. The beamformer ($\mathbf{W} \in \mathbb{C}^{M \times K}$) is defined as a matrix containing vectors $[\mathbf{w}_1, \mathbf{w}_2, \dots, \mathbf{w}_K]$, which each corresponds to an optimum value of beamforming coefficients at Tx for each Rx user.

The total received electric fields (\mathbf{E}) form a $T \times K$ matrix, with each column corresponding to the total received electric field associated at the T field points with a specific user's beamforming vector. This matrix is defined as a combination of the communication channel matrix $\tilde{\mathbf{H}} \in \mathbb{C}^{T \times M}$ and the beamforming matrix \mathbf{W} , according to [2]

$$\mathbf{E} = \tilde{\mathbf{H}}\mathbf{W} = \left\{ \mathbf{H}_u + \mathbf{G}_l^{\text{RT}} [\text{diag}(\mathbf{Z}_{\text{loads}}) - \mathbf{G}_{ll}]^{-1} \mathbf{H}_0 \right\} \mathbf{W}. \quad (1)$$

Here, $\mathbf{H}_u \in \mathbb{C}^{T \times M}$ represents the sub-channel matrix capturing the contributions from the TxS and the unloaded RIS to the field points. Similarly, $\mathbf{H}_0 \in \mathbb{C}^{N \times M}$ denotes the sub-channel matrix between the TxS and the RIS load elements, incorporating the effects of the unloaded RIS structure, including the dielectric substrate, top and bottom conducting layers [8]. Both matrices, \mathbf{H}_u and \mathbf{H}_0 , account for environmental interactions to ensure accurate modeling. The term $\mathbf{G}_l^{\text{RT}} \in \mathbb{C}^{T \times N}$ represents the electric field response at the observation points, as indicated by the orange dots in Fig. 1, due to currents induced at the load locations on the RIS. This matrix includes not only the effects of the tunable loads but also contributions from structural components, as well as environmental factors. The equivalent impedance of the tunable loads on the RIS is denoted by $\mathbf{Z}_{\text{loads}} \in \mathbb{C}^{N \times 1}$, while $\mathbf{G}_{ll} \in \mathbb{C}^{N \times N}$ accounts for the self- and mutual coupling among the load elements.

The primary objective is to maximize the minimum achievable rate (R_{\min}) while adhering to power constraints for each transmitting antennas. This is achieved through the co-optimization of the beamforming matrix (\mathbf{W}) and the tunable load impedances ($\mathbf{Z}_{\text{loads}}$) incorporated within the inverse non-diagonal impedance matrix, $[\text{diag}(\mathbf{Z}_{\text{loads}}) - \mathbf{G}_{ll}]^{-1}$, as detailed in (1). Unlike the phase-shifter approach [3], where the RIS is modeled as a simple diagonal phase-shifting matrix that controls the electric field $|\mathbf{E}|$ through a straightforward matrix-vector product, the model proposed in this paper provides a more comprehensive representation of RIS scattering behavior. It explicitly incorporates mutual coupling effects and systematically establishes the relationship between tunable load impedances and channel matrices. To this end, we assume a constant signal-to-noise ratio (SNR), with the noise power denoted as σ_0^2 , determined by the received signal strength at the target user. Additionally, interference is defined as the power received by unintended users, which we aim to minimize. The achievable rate, serving as the performance metric, is defined as [9]

$$R_k = \log_2 \left(1 + \frac{|E_{kk}(\mathbf{w}_k, \mathbf{Z}_{\text{loads}})|^2}{\sum_{j \neq k} |E_{kj}(\mathbf{w}_j, \mathbf{Z}_{\text{loads}})|^2 + \sigma_0^2} \right), \quad (2)$$

where \mathbf{w}_k is the beamforming vector designed to maximize the achievable rate for the k^{th} user. The term $|E_{kj}|$ represents the signal strength received by the k^{th} user due to the beamforming for the j^{th} user, while $|E_{kk}|$ denotes the strength of the desired signal at the k^{th} user. In this formulation, the numerator, $|E_{kk}|^2$, quantifies the power of the desired signal received at the k^{th} user. The denominator, $\sum_{j \neq k} |E_{kj}|^2 + \sigma_0^2$, captures the

combined effects of interference from the other $K - 1$ users, and the noise power.

The maximization of the overall objective (i.e., the minimum achievable rate across the users) is subject to two constraints. First, each Tx antenna is subject to a power constraint, denoted by P_m , ensuring that the transmitted power from each antenna does not exceed this limit. Second, the imaginary part of the load impedance is constrained to be within a specific range, which reflects the physical limitations of the impedance elements in the RIS. These two constraints guide the formulation of the optimization problem as follows

$$\begin{aligned} \max_{\mathbf{W}, \mathbf{Z}_{\text{loads}}} \quad & f(\mathbf{W}, \mathbf{Z}_{\text{loads}}) = \min_k \{R_k(\mathbf{W}, \mathbf{Z}_{\text{loads}})\} \\ \text{s.t.} \quad & \sum_{k=1}^K |w_{k,m}|^2 = P_m, \quad \forall m \in \{1, 2, \dots, M\}, \\ & Z_{\min} \leq \Im\{\mathbf{Z}_{\text{loads}}[n]\} \leq Z_{\max}, \quad \forall n \in \{1, 2, \dots, N\}, \end{aligned} \quad (3)$$

where $w_{k,m}$ specifies the weight of the m^{th} Tx antenna in the beamforming vector \mathbf{w}_k . To solve the problem, we adopt an alternating optimization strategy [9], which iteratively optimizes the beamforming vector and the tunable load impedance within the non-diagonal impedance matrix. The alternating optimization process for maximum minimum-rate is outlined in Algorithm 1. In this work, we utilize MATLAB's built-in optimization routine, 'fmincon', which is a gradient-based optimization tool designed to solve non-linear optimization problems.

Algorithm 1 Minimum-Rate Maximization Algorithm

- 1: **Input:** Sub-channel matrices \mathbf{H}_u and \mathbf{H}_0 ; Green's matrices \mathbf{G}_l^{RT} and \mathbf{G}_{ll} ; power constraints for transmitting antennas \mathbf{P} .
 - 2: **Initialize:** RIS configuration $\mathbf{Z}_{\text{loads}} \in \mathbb{C}^{N \times 1}$; beamforming matrix $\mathbf{W} \in \mathbb{C}^{M \times K}$.
 - 3: **while** not converged **do**
 - 4: Optimize $\mathbf{Z}_{\text{loads}}$ with fixed \mathbf{W} to maximize R_{\min} , subject to the imaginary part of $\mathbf{Z}_{\text{loads}}$ being constrained within $[Z_{\min}, Z_{\max}]$.
 - 5: Optimize \mathbf{W} with updated $\mathbf{Z}_{\text{loads}}$ to maximize R_{\min} , subject to power constraints \mathbf{P} for the transmitting antennas.
 - 6: **end while**
 - 7: **return** Optimized RIS configuration $\mathbf{Z}_{\text{loads}}$ and beamforming matrix \mathbf{W} .
-

III. SIMULATION RESULTS

TABLE I: MIMO communication system achievable rate (bps/Hz)

| Receiving locations | No RIS | With RIS deployed |
|---------------------|--------|-------------------|
| (1.30, 3.13, 0) m | 1.9174 | 2.5126 |
| (1.80, 2.38, 0) m | 1.9174 | 2.5121 |
| (2.30, 1.63, 0) m | 1.9174 | 2.5121 |

In this work, we conduct a MIMO communication example with three Tx's and three targeted users operated at 5.8 GHz as shown in Fig. 1. The Tx's are linear, single-polarized along the z -direction and positioned at (6, -3, 0) m. They are spaced $\lambda/2$ apart at the operating frequency. Each user is assumed to be equipped with a single antenna. However, the methodology presented in this work can also be extended to multi-user MIMO systems where both the users and the BS are equipped with multiple antennas. The RIS structure is identical to the one proposed in [2], where varactor diodes serve as tunable load elements, with capacitance values constrained between 0.2 and 0.9 pF. As a result, the load impedances ($\mathbf{Z}_{\text{loads}}$) are determined by the corresponding capacitance values (\mathbf{C}_{var}). The RIS is centrally positioned at (0, 0, 0) with dimensions of 0.533×0.331 m and oriented parallel to the yz -plane. It consists of 20×11 unit cells, each spaced by $\lambda/2$ at the operating frequency. Each unit cell contains two reconfigurable elements, resulting in a total of 440 varactors distributed across the surface. The RIS is controlled along one dimension (1D), where each column of unit cells have the same states. The three target users are located at (1.3, 3.13, 0) m; (1.8, 2.38, 0) m; and (2.3, 1.63, 0) m denoted as red circles in the Fig. 1. Since we have three users, the beamforming matrix can be written as

$$\mathbf{W} = [\mathbf{w}_1, \mathbf{w}_2, \mathbf{w}_3] = \begin{bmatrix} w_{1,1} & w_{2,1} & w_{3,1} \\ w_{1,2} & w_{2,2} & w_{3,2} \\ w_{1,3} & w_{2,3} & w_{3,3} \end{bmatrix}. \quad (4)$$

Furthermore, we assume a 1 W (30 dBm) power constraint (6) for each Tx antenna, with an SNR of 30 dB at each target user. The optimization problem can be formulated as

$$\max_{\mathbf{W}, \mathbf{C}_{\text{var}}} \quad f(\mathbf{W}, \mathbf{C}_{\text{var}}) = \min_k \{R_k(\mathbf{W}, \mathbf{C}_{\text{var}})\} \quad (5)$$

$$\text{s.t.} \quad \sum_{k=1}^3 |w_{k,m}|^2 = 1, \quad \forall m, \quad (6)$$

$$0.2 \leq \mathbf{C}_{\text{var}}[n] \leq 0.9 \text{ pF}, \quad \forall n. \quad (7)$$

The optimization results are presented and compared under two distinct scenarios: without RIS and with the optimized RIS deployed. In both cases, the beamforming matrix is optimized. The results are summarized in TABLE I. Furthermore, Fig. 2(a) depicts the total electric field distribution, \mathbf{E} , across the receiving region for the optimized RIS configuration, with the optimized beamforming matrix represented on a decibel-milliwatt (dBm) scale. Fig. 2(b)-(d) illustrate the signal strength corresponding to each beamforming vector, tailored for individual users and combined with the optimized RIS configuration. Notably, as the figures shown, the second user experiences the lowest signal strength, which is reasonable due to the influence of power constraints on each Tx antenna, indirectly shaping the signal distribution through the beamforming weights. Observe also that the beamformers tend to suppress the electric field strengths at the locations of the users they do not serve, which has the desired effect of minimizing interference. While the signal and interference

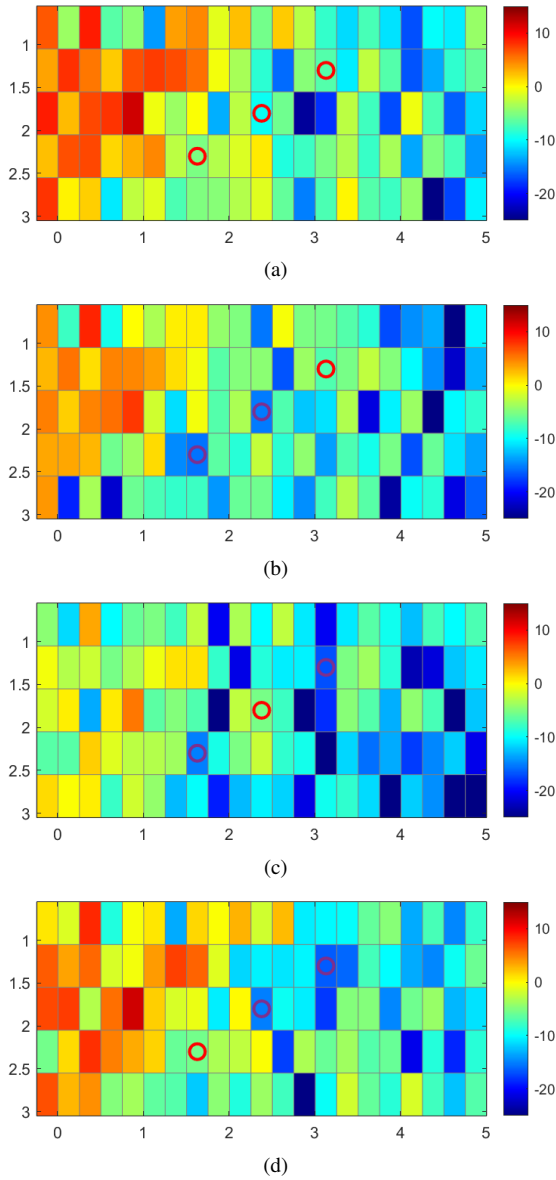


Fig. 2: Total electric fields ($|E|$ in dBm) within the region of interest in the presence of the optimized RIS highlighting 3 user locations: (1.30, 3.13, 0) m, (1.80, 2.38, 0) m, and (2.30, 1.63, 0) m marked by the red circles. The plots show (a) the total E-field with all beamforming vectors summed together and (b)-(d) the E-field distribution for the first, second, and third beamformers individually active.

strengths vary across the users, the achievable rates remain well-balanced. This aligns with the objective of maximizing the minimum achievable rate to ensure fairness among all users. The optimized beamforming matrix is

$$\mathbf{W} = \begin{bmatrix} 0.63 \angle -17.42^\circ & 0.42 \angle 117.67^\circ & 0.65 \angle -1.83^\circ \\ 0.55 \angle 19.13^\circ & 0.48 \angle 117.57^\circ & 0.68 \angle 89.72^\circ \\ 0.40 \angle -2.02^\circ & 0.48 \angle 89.26^\circ & 0.78 \angle -143.81^\circ \end{bmatrix}. \quad (8)$$

The optimized varactor capacitance values, arranged from the left to the right columns of the surface, are: [0.61 0.74 0.34

0.79 0.52 0.68 0.73 0.82 0.28 0.29 0.29 0.85 0.86 0.85 0.37 0.35 0.33 0.53 0.60 0.67] pF. The achievable rate shows a consistent improvement through the alternating optimization scheme, rising from approximately 1.91 bps/Hz to 2.51 bps/Hz across the three users with the deployment of the optimized RIS. The key parameters in (1) can be precomputed and reused during the optimization process. This eliminates the need for additional simulations in subsequent optimization iterations, significantly reducing computational overhead.

IV. CONCLUSION

This work presents an effective alternating optimization framework for maximizing the minimum achievable rate in MIMO communication systems by optimizing both the beamforming matrix and RIS configuration using deterministic channel information, derived through a hybrid RT and full-wave analysis approach. A non-diagonal impedance matrix is employed to account for mutual coupling, making the RIS model closer to practical performance. A comparative analysis of scenarios with and without RIS deployment demonstrates the significant improvement in achievable rates for all users. These results validate the potential of the proposed optimization scheme to enhance MIMO system performance. Future work include experimental validation, extending this work to millimeter-wave (mmWave) frequency bands and developing advanced optimization techniques that jointly optimize the RIS configuration and beamforming matrix to address nonlinear optimization challenges effectively.

REFERENCES

- [1] L. Dai, B. Wang, M. Wang, X. Yang, J. Tan, S. Bi, S. Xu, F. Yang, Z. Chen, M. D. Renzo, C.-B. Chae, and L. Hanzo, "Reconfigurable intelligent surface-based wireless communications: Antenna design, prototyping, and experimental results," *IEEE Access*, vol. 8, pp. 45913–45923, 2020.
- [2] Z. Liu, M. Behdani, and S. V. Hum, "Hybrid RT-MoM approach for RIS-enabled communication channel analysis and optimization in realistic environments," in *2024 IEEE Int. Symp. Antennas Propag. USNC-URSI Radio Sci. Meeting*, 2024, pp. 1217–1218.
- [3] R. Li, B. Guo, M. Tao, Y.-F. Liu, and W. Yu, "Joint design of hybrid beamforming and reflection coefficients in RIS-aided mmWave MIMO systems," *IEEE Trans. Commun.*, vol. 70, no. 4, pp. 2404–2416, 2022.
- [4] S. Kayraklik, I. Yildirim, I. Hokelek, Y. Gevez, E. Basar, and A. Gorcin, "Indoor measurements for RIS-aided communication: Practical phase shift optimization, coverage enhancement, and physical layer security," *IEEE Open J. Commun. Soc.*, vol. 5, pp. 1243–1255, 2024.
- [5] Q. Wu and R. Zhang, "Intelligent reflecting surface enhanced wireless network via joint active and passive beamforming," *IEEE Trans. Wireless Commun.*, vol. 18, no. 11, pp. 5394–5409, 2019.
- [6] J. He, H. Wymeersch, and M. Juntti, "Channel estimation for RIS-aided mmWave MIMO systems via atomic norm minimization," *IEEE Trans. Wireless Commun.*, vol. 20, no. 9, pp. 5786–5797, 2021.
- [7] Y. Liu, Z. Liu, S. V. Hum, and C. D. Sarris, "Numerical modeling and experimental validation of path loss in realistic RIS-enabled links," in *2023 IEEE Int. Symp. Antennas Propag. USNC-URSI Radio Sci. Meeting*, 2023, pp. 451–452.
- [8] S. K. R. Vuyyuru, R. Valkonen, S. A. Tretyakov, and D.-H. Kwon, "Efficient synthesis of large finite patch arrays for scanning wide-angle anomalous reflectors," *IEEE Open J. Antennas Propag.*, pp. 1–1, 2024.
- [9] H. Xie, J. Xu, and Y.-F. Liu, "Max-min fairness in IRS-aided multi-cell MISO systems with joint transmit and reflective beamforming," *IEEE Trans. Wireless Commun.*, vol. 20, no. 2, pp. 1379–1393, 2021.